J. Fluid Mech. (1983), *vol.* 129, *pp.* 123–136
Printed in Great Britain

On the propagation of weak and moderately strong, curved shock waves

By FRANK OBERMEIER
Max-Planck-Institut für Strömungsforschung, D-3400 Göttingen, Federal Republic of Germany

(Received 31 July 1982)

In this paper we concern ourselves with the theoretical description of curved converging shock waves, where nonlinear interaction effects, between the shock fronts and the flow behind them, and refraction effects are equally important. In a non-viscous, isoenergetic and isentropic flow the problem can be described by a nonlinear wave equation for the pressure field. This equation then admits an analytical solution with the help of the method of strained coordinates provided that the nonlinear terms contain only derivatives with respect to two independent variables. This restrictive condition is approximately fulfilled if the incoming wave is only slightly curved.

Replacing in the solution the strained coordinates – which themselves depend on the solution – by physical coordinates, we get an accurate description of the transition from the shock pattern obtained by the geometric-acoustics approach (very weak shocks) to the pattern determined by Whitham's shock dynamics (strong shocks). Furthermore, the solution describes the complete flow field and agrees very favourably with experimental data by Sturtevant & Kulkarny.

1. Introduction

Interest in shock propagation occurs in a variety of fields: well-known examples include the generation and propagation of sonic booms caused by supersonically flying aircraft, shock propagation in shock tubes in which different media are investigated under diverse flow conditions (including chemical reactions), and the phenomenon of thunder, to mention only a few. The propagation behaviour of weak shock-wave systems, and especially the interaction between single shocks of the system and the interaction between shocks and the flow field behind them, is still a very fascinating and only partly solved problem in fluid mechanics, despite the fact that basic results were already obtained more than 100 years ago. (A short survey of the most important achievements of the last century in nonlinear wave propagation can be found in a paper by Rott (1980).)

The main topic of the present paper is concerned with shock propagation of non-planar shock fronts. These waves easily occur when plane waves travel through inhomogeneous (for instance, layered) media or when the shock generation is time- and (or) space-dependent. Here, it is a well-established fact that a shock front, once curved, will, if concave, then converge as it propagates, to form focal points or caustics, provided that the amplitude of the converging wave is sufficently small. As an illustrative example we may think of a sonic boom caused by manoeuvring aircraft.

In many cases the incoming shock front has a minimum radius of curvature R_0, which leads to a cusp in the caustic, also called an arête. A qualitative sketch showing

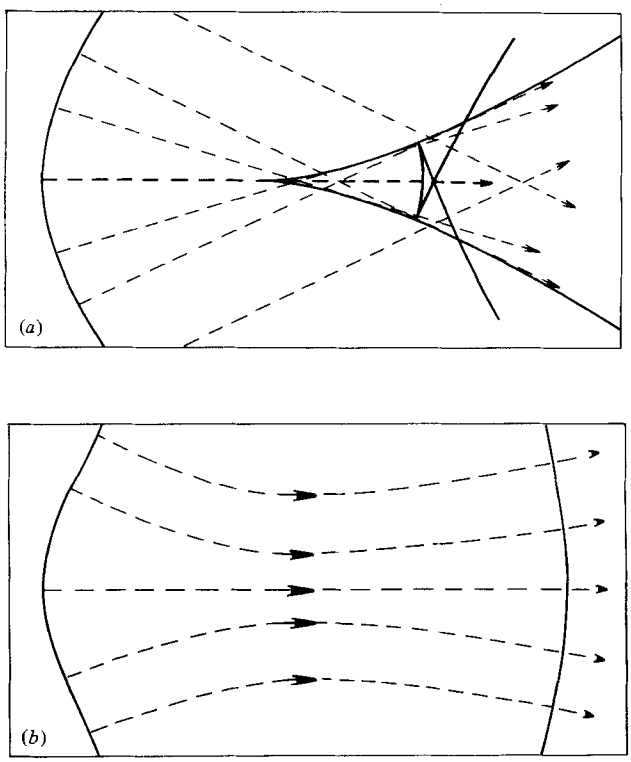

FIGURE 1. Propagation of converging shock waves: (*a*) according to geometric acoustics, (*b*) according to shock dynamics (Whitham). ——, shock waves; ——, caustic; – – –, rays.

the development of such a cusped caustic is reproduced in figure 1 (*a*). Here, within the framework of geometric acoustics, caustics are understood as the envelopes of converging ray tubes. This representation describes sufficiently accurately the flow pattern; however, it does not allow for an estimation of the actual pressure amplitude near the caustic, because a geometric wave theory implies zero differential cross-sections of the ray tubes at the caustic, and thereby leads to infinitely large pressure values. Furthermore, such a theory would predict no pressure variation at all of a focused wave outside the two branches of the caustic. Pressure distributions which actually occur near a caustic were measured, for instance, by Vallee (1969) (see also Wanner *et al.* 1972).

If the amplitude of the incoming concavely curved wave is no longer small, a quite different pattern of the shock location will be displayed, like that plotted in figure 1 (*b*). This field may be explained by a modified ray theory – also called Whitham's shock dynamics. It takes into account that the propagation speed of a shock front increases with increasing shock strength, while the propagation direction of the wave remains always normal to its front. These two effects turn the shock front and bend the rays, and therefore prevent the crossing of ray tubes. A detailed theoretical investigation of shock dynamics was given by Whitham (1957, 1959, 1974).

Unfortunately, both of the geometric theories touched on above neither account for nonlinear interactions between shock fronts and the flow behind them nor account for refraction effects, which turn out to be equally important for the calculation of the actual pressure time history. Therefore the theories are not really suitable for a

satisfactory investigation of flow fields with weak, or moderately strong, non-planar shock waves.

First attempts to overcome the difficulties related to infinite peak overpressures obtained by geometric acoustics were very similar to those of 'boundary-layer' theories (Lighthill 1950; Buchal & Keller 1960). There the flow field is divided into two regions: the first is the region outside the vicinity of the caustic in which geometric theories can be applied and yield reasonable results, and the second is the region near the caustic itself – the so-called boundary-layer region – in which the equations of motion are reduced to modified transonic differential equations. The asymptotically valid equations of motion for these 'outer' and 'inner' regions can then be solved, at least in principle, by using the method of matched asymptotic expansions.

Progressing along that line, Guiraud (1965), Hayes (1968), and Seebass (1971) proposed 'transonic' theories. Their basic idea was to introduce a coordinate system whose origin moves with the velocity $a_0 \mathbf{n}$ (a_0 is the speed of sound and $\mathbf{n}$ is the normal vector of the incoming wave at the caustic) along the caustic. In this coordinate system the flow turns out to be, with restrictions, a steady transonic flow field. The focusing of shock waves now appears as a reflection of shock waves at the sonic line. Unfortunately, the corresponding solutions obtained by Seebass for the modified transonic equations reveal certain unrealistic properties. In the physical plane the solutions do not cover the entire flow field, but leave a 'gap' at the front of the incoming signal. For this flow region, additional assumptions were therefore necessary. A detailed discussion of the problem and its roots, and a method to get improved solutions of the transonic equations, were given by Obermeier (1976).

In 1978, Cramer & Seebass took up the problem of focused shock waves again. On the basis of the nonlinear wave equation for an unsteady potential flow, they derived a similarity law for very weak shock waves, which allows a determination of the dependence of the pressure levels and the amplification laws on the gas properties and on the initial shape and strength of the incoming shock. The method is only valid for extremely low shock strength; furthermore, an actual solution, expressing the time and space dependence of the flow field, has not been given yet.

Further solutions of the steady transonic equation were found by Fung (1980) for special pressure signatures of the incoming wave.

Systematic experimental investigations, carried out by Sturtevant & Kulkarny (1976), improved our understanding of converging flow fields considerably. Using shadowgraph techniques and pressure measurements, they studied the focusing behaviour of curved shock waves for a wide range of different geometries and for varying shock strength.

Stimulated by their results, we have developed a theoretical method which takes account of nonlinear effects as well as of refraction effects in a feasible approximation. The method will, in particular, allow an explanation of the transition from the limit of geometric acoustics to the state of moderately strong shock waves. It also gives a satisfactory explanation of the varying shock pattern as a function of the amplitude of the incoming shock waves, which was found experimentally by Sturtevant & Kulkarny (1976). Whitham's limit of shock dynamics itself (strong shocks) is not, however, covered by our approximation.

2. Basic equations and assumptions

Our investigation is based on the equations of an unsteady isentropic and isoenergetic flow, where viscosity effects are negligible. Additionally, we assume that the strength of the curved shock fronts is still small enough to justify neglect of gradients of entropy production behind the shock waves. Consequently, the flow field may be written in terms of a nonlinear wave equation for the flow potential φ:

$$\Delta\varphi - \frac{1}{a_0^2}\frac{\partial^2\varphi}{\partial t^2} = \frac{1}{a_0^2}\frac{\partial}{\partial t}\left\{(\nabla\varphi)^2 + \frac{\kappa-1}{2}\left(\frac{\partial\varphi}{\partial t}\right)^2\right\} + \text{cubic terms}. \tag{1}$$

Here a_0 is the speed of sound in the medium at rest, κ the ratio of specific heats, $\mathbf{x} = \{x_1, x_2, x_3\}$ is the space coordinate and t the time coordinate. In accordance with the neglect of entropy variations behind curved shock waves, terms of third order in (1) have been neglected, too.

To solve this equation, we need, in addition, boundary conditions. We therefore assume that the time history of the pressure of the incoming wave and its normal derivative is prescribed at a surface S (figure 2), which is sufficiently far away from the location where geometric wave theories predict a caustic. To be more precise, we require the lengthscale of the pressure signal to be small compared with the minimum radius of curvature R_0 of the surface S. In addition, outgoing waves have to fulfil – roughly speaking – Sommerfeld's radiation conditions. We will make the last condition explicit later on.

As the boundary conditions are given for the pressure field but not for the flow potential, it turns out to be preferable to replace (1) by an equation for the pressure field p defined by Bernoulli's equation:

$$p = \frac{1}{\kappa}\rho_0 a_0^2\left[1 - \frac{\kappa-1}{a_0^2}\left(\frac{\partial\varphi}{\partial t} + \tfrac{1}{2}(\nabla\varphi)^2\right)\right]^{\kappa/(\kappa-1)}, \tag{2}$$

where ρ_0 is the density of the medium at rest.

For the sake of simplicity, it is also reasonable to use non-dimensional variables throughout the succeeding calculations. Even though there is no unique way to select non-dimensional variables at the present stage, the discussions following later suggest as an appropriate choice:

$$\mathbf{x} = R_0\mathbf{X}, \quad t = \frac{R_0}{a_0}T, \quad \frac{\kappa p}{\rho_0 a_0^2} - 1 = \epsilon P, \quad \varphi = \epsilon\frac{a_0 R_0}{\kappa}\phi. \tag{3}$$

Here ϵ is the dimensionless maximum of the pressure amplitude of the unfocused signal at S. For a sonic boom a characteristic ϵ-value is of the order $\epsilon = 10^{-3}$ (corresponding to 100 N/m^2).

Introducing (2) and (3) into (1) yields

$$\Delta P - \frac{\partial^2 P}{\partial T^2} = -\frac{\epsilon}{2}\left[\frac{\partial^2 P^2}{\partial T^2} - \frac{1}{\kappa}\Delta P^2 + \frac{1}{\kappa}\left\{\frac{\partial^2(\nabla\phi)^2}{\partial T^2} + \Delta(\nabla\phi)^2\right\}\right] + O(\epsilon^2). \tag{4}$$

The last two terms, still depending on $(\nabla\phi)^2$, will be replaced by pressure terms later on.

The problem we are now faced with is the following. We have to solve a nonlinear wave equation for a converging flow field that includes shock waves. This flow field is governed by two distinct, competing effects: (i) the geometry of the shock pattern and (ii) a nonlinear interaction of the shock fronts with the flow behind them, known as the steepening effect. The well-understood plane waves are free of the first effect,

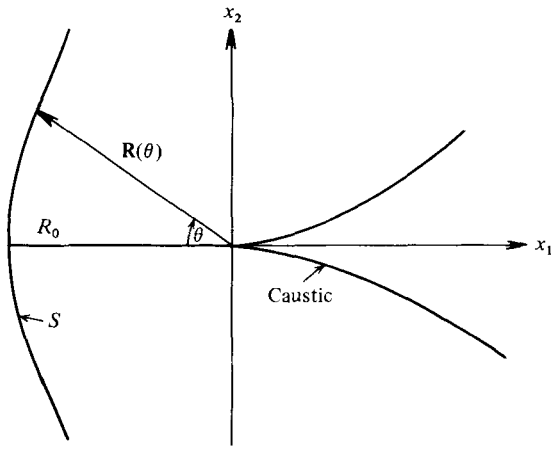

FIGURE 2. Coordinates and notation.

linear non-planar waves are free of the second. Solutions of (4) for flow fields where both effects are of comparable importance seem to be known only for highly symmetrical flow geometries, e.g. spherical flows. In all other cases approximations are necessary, which usually are based on the assumption that one of the two effects is overwhelmingly present and can be dealt with analytically, while the second effect plays a secondary role only and can be regarded as a perturbation of the first.

We assume here that the flow field in question can be viewed, in a first approximation, as a nonlinear plane wave and that the geometric effects play the role of perturbations. This approach requires that the incoming wave is only slightly curved and its normal vector **n** does not deviate very much from the main propagation direction, i.e. the X_1 axis: thus

$$\mathbf{n} = \{1 - \tfrac{1}{2}\theta^2 + \tfrac{1}{24}\theta^4,\ \theta - \tfrac{1}{6}\theta^3\}, \quad \theta_{\max} \ll 1. \tag{5}$$

Here θ is the angle between **n** and the X_1 axis; furthermore, we confine the investigations to two-dimensional flow fields only.

The condition (5) is equivalent to keeping those nonlinear terms in (4) that contain only derivatives with respect to X_1 and T, but ignoring nonlinear terms (not linear ones) that contain derivatives with respect to X_2. These approximations, which are equivalent to those commonly applied to derive the equation for the potential of an unsteady transonic flow, yield for propagating waves

$$\frac{\partial P}{\partial T} = -\frac{\partial P}{\partial X_1} + O(\epsilon, \theta_{\max}), \quad \frac{\partial \phi}{\partial T} = -\frac{\partial \phi}{\partial X_1} + O(\epsilon, \theta_{\max}), \quad \frac{\partial \phi}{\partial T} = -P + O(\epsilon).$$

Introducing these relations into (4) leads to a considerably simplified wave equation:

$$\Delta P - \frac{\partial^2 P}{\partial T^2} = -\epsilon \frac{\kappa+1}{4\kappa} \frac{\partial^2 P^2}{\partial T^2} + O(\epsilon^2, \epsilon\theta_{\max}), \tag{6}$$

In the same approximation, (2) simplifies to

$$P = -\phi_T + O(\epsilon^2, \epsilon\theta_{\max}),$$

which implies that (6) is equivalent to the transonic equation

$$\Delta\phi - \phi_{TT} = \epsilon \frac{\kappa+1}{2\kappa} \frac{\partial}{\partial T} (\phi_T)^2$$

or

$$\Delta\phi - \phi_{TT} = -\epsilon \frac{\kappa+1}{2\kappa} \frac{\partial}{\partial X_1} (\phi_{X_1})^2,$$

respectively. The less known equivalence between the latter two equations is valid because the difference between the nonlinear terms $\phi_{X_1}\phi_{X_1X_1}$ and $-\phi_T\phi_{TT}$ is of the same order of smallness as terms already neglected in deriving the transonic equations.

3. General solution

The basic ideas of the method of strained coordinates may be found in textbooks; therefore we confine our further explanations to the principal results. In a first step we introduce strained coordinates of the following form into (6):

$$T = \tilde{T} + \epsilon H(\tilde{T}, \tilde{\mathbf{X}}), \quad \mathbf{X} = \tilde{\mathbf{X}}. \tag{7}$$

Here H is an unknown function. To determine this function we require that (i) (6) becomes linear in terms of strained coordinates, and (ii) the strained and the physical coordinates coincide at the surface S. Both conditions have to be fulfilled up to $O(\epsilon^2, \epsilon\theta_{\max})$ in accordance with previous approximations.

We obtain

$$H = -\frac{\kappa+1}{2\kappa}(1+\tilde{X}_1)\, P(\tilde{T}, \tilde{\mathbf{X}}) + O(\epsilon, \theta_{\max}), \tag{8a}$$

$$\frac{\partial^2 P}{\partial \tilde{T}^2} - \tilde{\Delta} P = O(\epsilon^2, \epsilon\theta_{\max}). \tag{8b}$$

This result implies that we have succeeded in replacing the original nonlinear wave equation by a linear wave equation. Its corresponding solution is correct to $O(\epsilon^2, \epsilon\theta_{\max})$, i.e. nonlinear steepening effects with respect to the main flow direction ($\tilde{X}_1$ axis) and non-planar linear refraction effects are both taken into account.

To determine the solution P of (8b) we can transfer the boundary condition at the surface S from the physical to the strained coordinates, as both coordinates coincide at S. Furthermore, we require that those parts of the pressure P which represent outgoing linear waves in terms of strained coordinates, fulfil Sommerfeld's radiation condition.

Considering these boundary conditions and the assumption that the distance between the observation point $\mathbf{X}$ and the surface S is large compared with the length of the incoming signal, the complete solution can be expressed in terms of a double integral of the form (see Buchal & Keller 1960)

$$P(\tilde{T}, \tilde{\mathbf{X}}) = \frac{1}{2\pi} \int_S \int_{-\infty}^{\infty} \hat{P}_S(\omega) \left(\frac{\omega}{2\pi}\right)^{\frac{1}{2}} \frac{\exp i\left(\frac{\pi}{4} + \omega \left|\frac{\mathbf{R}(\theta)}{R_0} - \tilde{\mathbf{X}}\right| - \omega\tilde{T}\right)}{\left|\frac{\mathbf{R}(\theta)}{R_0} - \tilde{\mathbf{X}}\right|^{\frac{1}{2}}} d\omega\, dS, \tag{9a}$$

$$T = \tilde{T} - \epsilon \frac{\kappa+1}{2\kappa}(\tilde{X}_1 + 1)\, P(\tilde{T}, \tilde{\mathbf{X}}), \quad \mathbf{X} = \tilde{\mathbf{X}}, \tag{9b}$$

where $\hat{P}_S(\omega)$ is the Fourier transform of the incoming pressure signal at S:

$$\hat{P}_S(\omega) = \int_{-\infty}^{\infty} P_S(T)\, e^{i\omega T}\, dT.$$

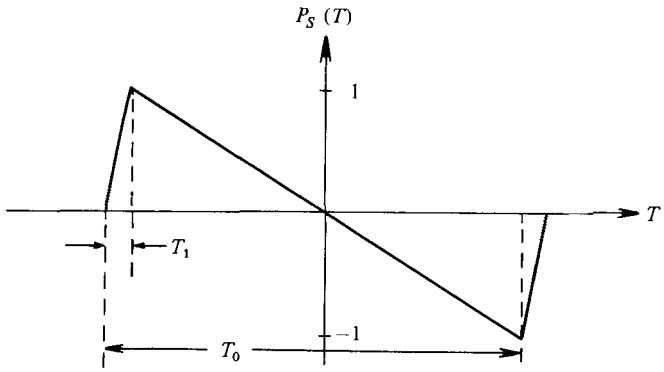

FIGURE 3. Pressure signature at the surface S with $10^{-4} \leqslant T_1/T_0 \leqslant 10^{-2}$; T_0, duration of the signal; T_1, shock-rise time.

To evaluate the implicitly given solution of (9) we first have to specify the surface S and the time history of the pressure $P_S(T)$. To that end we assume

$$S(\tilde{X}_1, \tilde{X}_2): \begin{cases} \tilde{X}_1^S = -(1+\beta|\theta|^3)\cos\theta, \\ \tilde{X}_2^S = (1+\beta|\theta|^3)\sin\theta, \end{cases}$$

where $\beta > 0$ is a free parameter. The form of S agrees qualitatively with the shape of the converging shock waves investigated experimentally by Sturtevant & Kulkarny (1976); quantitative differences are mainly caused by our restriction that S is only slightly curved.

Furthermore, as the numerical evaluation of the integral (9) (including the determination of the Fourier transform) is still difficult for an arbitrary pressure signature $P_S(T)$ of the incoming wave, we restrict the investigation to N-waves with short but finite rise time T_1 (figure 3). The slightly unusual assumption of a finite shock-rise time is justified as one has to keep in mind that from a physical point of view there are no relevant differences whether we choose $T_1 > 0$ or $T_1 = 0$ at S as a boundary condition, provided that T_1 is sufficiently small in accordance with measured data. The only appropriate questions that could arise are the following. (i) Does the solution based on $T_1 > 0$ at S exhibit unrealistic pressure signatures at any point of the flow field? (ii) Are there any significant differences in terms of real coordinates between a solution based on $T_1 > 0$ and a solution based on $T_1 = 0$? The answers are 'no' in both cases; differences occur only in terms of strained coordinates, as we will explain later on.

In a next step we evaluate the integral equation (9.1) in terms of strained coordinates. The main problem we are still left with is the oscillatory phase factor $\exp i\omega\,|\mathbf{R}(\theta)/R_0 - \tilde{\mathbf{X}}|$ of its integrand. For this reason an ordinary numerical determination of the integral seems to be rather hopeless, and we have to apply asymptotic methods. These calculations are confined in the present paper to a few typical locations in the $\tilde{\mathbf{X}}$-plane, which, however, will already allow a discussion of the entire flow field. Furthermore, as the flow field is symmetric with respect to the $\tilde{X}_1$ axis, we consider only the upper half-plane, with $\tilde{X}_2 \geqslant 0$.

(i) $\tilde{\mathbf{X}} = 0$, *which corresponds to the location of the cusp of the caustic*. Here the general integral (9*a*) simplifies to

$$P(\tilde{T}, 0) = \frac{1}{\pi}\int_0^\infty \int_{-\infty}^\infty \hat{P}_S(\omega)\frac{|\omega|^{\frac{1}{6}}}{(2\pi)^{\frac{1}{2}}}\left(1 - \frac{3\xi^3}{2\omega}\right) e^{i(\frac{1}{4}\pi + \omega - \omega\tilde{T})}\beta^{-\frac{1}{3}} e^{i\xi^3} d\omega\, d\xi, \tag{10}$$

with $\xi = |\beta\omega|^{\frac{1}{3}}\theta$. Neglecting the second term of the sum and performing the ξ-integration we obtain

$$P(\tilde{T},0) = \frac{1}{2\pi}(2^3\pi)^{\frac{1}{2}}\left(\frac{1}{3\beta}\right)^{\frac{1}{3}}\int_{-\infty}^{\infty}\hat{P}_S(\omega)\,|\omega|^{\frac{1}{6}}\,[\mathrm{Ai}\,(0)+i0{\cdot}231\ \mathrm{Bi}\,(0)]\,e^{i(\frac{1}{4}\pi+\omega-\omega\tilde{T})}\,dw, \quad (11)$$

where Ai (z), Bi (z) are Airy functions with Ai $(0) = 0{\cdot}355$ and Bi $(0) = 0{\cdot}615$.

The result means that each Fourier component of the incoming wave $\hat{P}_S(\omega)$ has to be multiplied by

$$\frac{2^{\frac{3}{2}}\pi^{\frac{1}{2}}}{(3\beta)^{\frac{1}{3}}}|\omega|^{\frac{1}{6}}\,A\,e^{i(\frac{1}{4}\pi+\gamma)},$$

where $A = [\mathrm{Ai}\,(0)^2 + (0{\cdot}231\ \mathrm{Bi}\,(0))^2]^{\frac{1}{2}}$ and $\gamma = \arctan[0{\cdot}231\ \mathrm{Bi}\,(0)/\mathrm{Ai}\,(0)]$.

(ii) $\tilde{\mathbf{X}}$ *well within the area bounded by the two branches of the caustic. The caustic itself and its immediate vicinity are excluded.* In this area (named A) the phase function $E = |\mathbf{R}(\theta)/R_0 - \tilde{\mathbf{X}}|$ has three distinct, simple extrema in correspondence with three separated waves found by geometric acoustics in A. Thus it turns out that the method of steepest descent yields reasonable asymptotic approximations of $(9a)$. Passing over the details of the algebra, we obtain

$$P(\tilde{T},\tilde{\mathbf{X}}_A) = \frac{1}{2\pi}\sum_{\nu=1}^{3}(1-\beta|\theta_{St}^{(\nu)}|^3)\left[\frac{2}{|F''(\theta_{St}^{(\nu)})|}\right]^{\frac{1}{2}}$$

$$\times\int_{-\infty}^{\infty}\hat{P}_S(\omega)\exp\left[i\tfrac{1}{4}\pi(1-\operatorname{sgn}E''(\theta_{St}^{(\nu)},\tilde{\mathbf{X}}_A)) + i\omega(E(\theta_{St}^{(\nu)},\tilde{\mathbf{X}}_A)-\tilde{T})\right]d\omega, \quad (12)$$

where

$$F(\theta) = (E(\theta,\tilde{\mathbf{X}}_A))^2, \quad \theta_{St}:\{F'(\theta)=0\},$$

$$F''(\theta) = -2\tilde{X}_{1A} + 2[\tilde{X}_{2A} \pm 12\beta(1+\tilde{X}_{1A})]\,\theta + (\tilde{X}_{1A} \mp 24\beta\tilde{X}_{2A})\theta^2 + O(\theta^3);$$

the upper sign is valid if $\theta_{St} > 0$, the lower sign if $\theta_{St} < 0$.

In this case the Fourier components are multiplied by a factor that does not depend on the frequency ω. Furthermore, the phase shift is zero for the incoming signals and $\frac{1}{2}\pi$ for the outgoing, the focused signal.

(iii) *Along the upper branch of the caustic* ($\tilde{\mathbf{X}}_c$) *and in its vicinity.* Considering the flow in a vicinity of a point $\tilde{\mathbf{X}}_c$ located on the caustic, its behaviour is determined by two contributions P_1 and P_2. One is due to the incoming wave, which again is asymptotically given by the method of steepest descent as

$$P_1(\tilde{T},\tilde{\mathbf{X}}) = \frac{1}{2\pi}\left[\frac{2}{|F''(\theta_{St}^{(1)})|}\right]^{\frac{1}{2}}\int_{-\infty}^{\infty}\hat{P}_S(\omega)\exp i\omega(E(\theta_{St}^{(1)},\tilde{\mathbf{X}})-\tilde{T})\,d\omega, \quad (13a)$$

where

$$\theta_{St}^{(1)}: F'(\theta_{St},\tilde{\mathbf{X}}_c) = 0,\ F''(\theta_{St},\tilde{\mathbf{X}}_c) \neq 0,\ \theta_{St} > 0\}, \quad |\tilde{\mathbf{X}}-\tilde{\mathbf{X}}_c| \ll 1.$$

The second contribution $P_2(\tilde{T},\tilde{X})$ is given by an expansion of the part of the integrand in $(9a)$ that represent the focused signal in $\tilde{\mathbf{X}}$ if $\tilde{\mathbf{X}}$ is in the vicinity of a point $\tilde{\mathbf{X}}_c$ on the caustic ($|\tilde{\mathbf{X}}-\tilde{\mathbf{X}}_c| \ll 1$), i.e. if the two extreme $\theta_{St}^{(2)}$ and $\theta_{St}^{(3)}$ considered in (ii) coalesce:

$$P_2(\tilde{T},\tilde{\mathbf{X}}) \approx \frac{1}{2\pi}\int_{-\infty}^{\infty}\hat{P}_S(\omega)\left(\frac{\omega}{2\pi}\right)^{\frac{1}{2}}\int_{-\infty}^{\infty}\frac{1}{|E(\theta_{St}^{(2)},\tilde{\mathbf{X}}_c)|^{\frac{1}{2}}}\exp\left[i\tfrac{1}{4}\pi + i\omega E(\theta_{St}^{(2)},\tilde{\mathbf{X}})\right]$$

$$\times\exp\{i\omega[E'(\theta_{St}^{(2)},\tilde{\mathbf{X}})\,\xi + E''(\theta_{St}^{(2)},\tilde{\mathbf{X}})\,\tfrac{1}{2}\xi^2 + E'''(\theta_{St}^{(2)},\tilde{\mathbf{X}})\,\tfrac{1}{6}\xi^3] - i\omega\tilde{T}\}\,d\xi\,d\omega,$$

where

$$\theta_{St}^{(2)}: \{E'(\theta,\tilde{\mathbf{X}}_c) = 0,\ E''(\theta,\tilde{\mathbf{X}}_c) = 0,\ E(\theta,\tilde{\mathbf{X}}_c) \neq 0,\ \theta < 0\}, \quad \xi = \theta_{St}^{(2)} - \theta.$$

By means of the transformation

$$\xi = \xi - \frac{2E''(\theta_{St}, \tilde{\mathbf{X}})}{E'''(\theta_{St}, \tilde{\mathbf{X}})}$$

we obtain

$$P_2(\tilde{T}, \tilde{\mathbf{X}}) = \frac{1}{2\pi}\int_{-\infty}^{\infty} \hat{P}_S(\omega)\left(\frac{2\omega}{\pi}\right)^{\frac{1}{2}} \frac{e^{i(\frac{1}{4}\pi + \omega A - \omega\tilde{T})}}{|E(\theta_{St}^{(2)}, \tilde{\mathbf{X}}_c)|^{\frac{1}{2}}} \int_0^{\infty} \cos(\omega B\xi + \omega C\xi^3)\, d\xi\, d\omega,$$

with

$$A = \left[E - \frac{E'E''}{E'''} + \frac{1}{3}\frac{E'^3}{E'''^2}\right]_{\theta_{St}^{(2)}, \tilde{\mathbf{X}}},$$

$$B = \left[E' - \frac{1}{2}\frac{E''^2}{E'''}\right]_{\theta_{St}^{(2)}, \tilde{\mathbf{X}}},$$

$$C = [\tfrac{1}{6}E''']_{\theta_{St}^{(2)}, \tilde{\mathbf{X}}}.$$

This integral can be expressed by Airy functions (or by Bessel functions of order $\frac{1}{3}$ (see e.g. Abramowitz & Stegun 1964):

$$P_2(\tilde{T}, \tilde{\mathbf{X}}) = \left[\frac{2\pi}{E(\theta_{St}^{(2)}, \mathbf{X}_c)}\right]^{\frac{1}{2}} \frac{e^{i\frac{1}{4}\pi}}{(3C)^{\frac{1}{3}}} \frac{1}{2\pi}\int_{-\infty}^{\infty} |\omega|^{\frac{1}{6}} \mathrm{Ai}\left(\frac{|\omega|^{\frac{1}{6}}B}{(3C)^{\frac{1}{3}}}\right) \hat{P}_S(\omega)\, e^{i\omega(A-\tilde{T})}\, d\omega. \quad (13b)$$

Here the main result is that the Fourier components decay exponentially for $B > 0$, in fact increasing with growing frequency ω.

For $\mathbf{X} = \mathbf{X}_c$, i.e. at the caustic, where $E'(\theta_{St}^{(2)}, \tilde{\mathbf{X}}_c) = E''(\theta_{St}^{(2)}, \tilde{\mathbf{X}}_c) = 0$, the contribution P_2 simplifies to

$$P_2(\tilde{T}, \tilde{\mathbf{X}}_c) = \frac{2^{\frac{7}{6}}\pi^{\frac{1}{2}}}{|F'''(\theta_{St}^{(2)})|^{\frac{1}{3}}} \frac{1}{E(\theta_{St}^{(2)})^{\frac{1}{6}}} \mathrm{Ai}(0)\, e^{i\frac{1}{4}\pi}$$

$$\times \frac{1}{2\pi}\int_{-\infty}^{\infty} \hat{P}_S(\omega)\, |\omega|^{\frac{1}{6}} \exp i\omega[E(\theta_{St}^{(2)}, \tilde{\mathbf{X}}_c) - \tilde{T}]\, d\omega, \quad (13c)$$

where

$$F'''(\theta_{St}^{(2)}) = 2[\tilde{X}_{2c} - 6\beta(1 + \tilde{X}_{1c})] + 2(\tilde{X}_{1c} + 24\beta\tilde{X}_{2c})\,\theta_{St}^{(2)}$$
$$+ (\tilde{X}_{2c} + 60\beta\tilde{X}_{1c})\,(\theta_{St}^{(2)})^2 + O((\theta_{St}^{(2)})^3).$$

4. Numerical results

4.1. *Strained coordinates*

The asymptotic solutions in terms of an inverse Fourier transform, (11)–(13), derived in §3, can now be evaluated numerically. The most interesting results are summarized in figure 4.

We find the following:

(i) The shape of the incoming signal remains nearly unchanged outside the region bounded by the cusp and the two branches of the caustic.

(ii) Refraction effects, which are included in our linear wave theory (but are not included in a geometric wave theory), limit the amplification of the focused signal and yield the typical signatures of a focused pressure distribution: a sharp peak followed by a strong expansion.

(iii) The pressure amplitude is finite at the caustic and the amplification of the pressure behaves approximately like $(T_1/T_0)^{-\frac{1}{4}}$ for $10^{-4} \leqslant T_1/T_0 \leqslant 10^{-2}$ (see figure 5); details of these calculations are included in Obermeier (1976). Physically it means that the amplification is only weakly dependent on the rise time. However, it is also known that for an idealized rise time $T_1 = 0$ the signature of a focused signal has

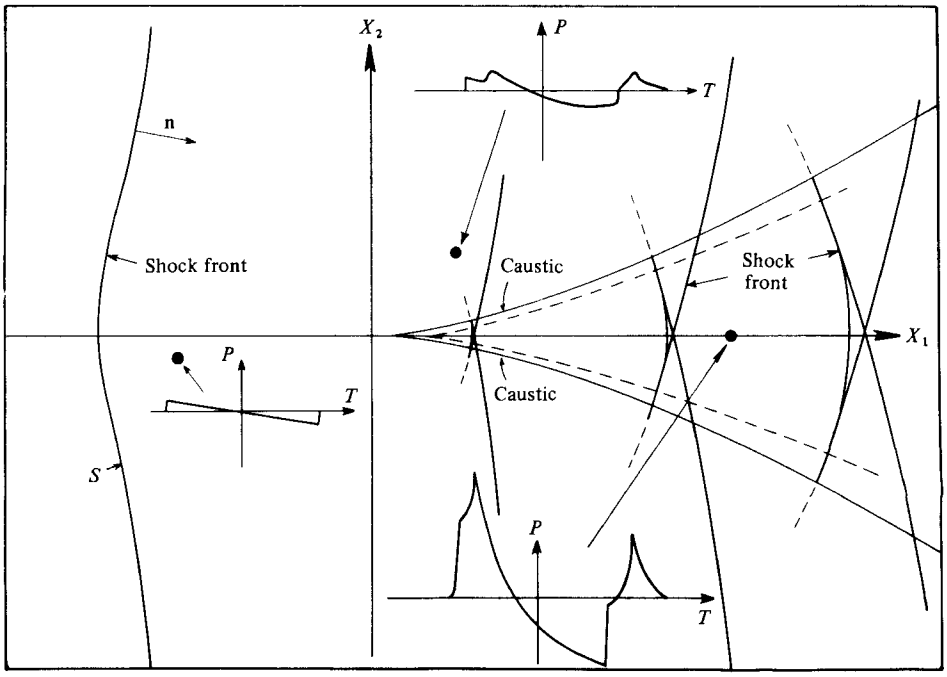

FIGURE 4. Summarized results according to the method of strained coordinates.

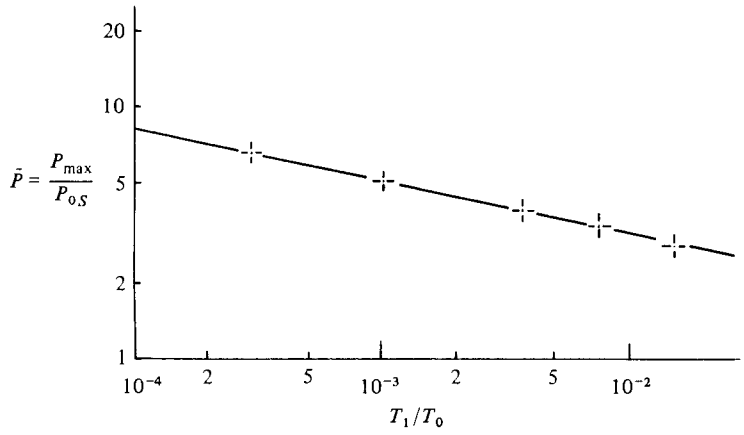

FIGURE 5. Amplification $P = P_{max}/P_{0S}$ as a function of the shock-rise time T_1; T_0 duration of the N-wave.

singularities at the front and the rear shock. As we will show later, these singularities occur only in strained coordinates, but do not really affect the solution in terms of physical coordinates.

(iv) The maximum amplification does not occur at the caustic but somewhat below (or above, respectively), as indicated by the dashed lines in figure 4. This result is explained by the fact that each single Fourier component of the solution is expressed in terms of Airy functions $\mathrm{Ai}(|\omega|^{\frac{1}{6}}B/(3C)^{\frac{1}{3}})$ which take their maximum value at $|\omega|^{\frac{1}{6}}B/(3C)^{\frac{1}{3}} \approx 1$, but not at the caustic ($B = 0$). Furthermore, in the immediate vicinity of the caustic the incoming converging waves are converted by refraction

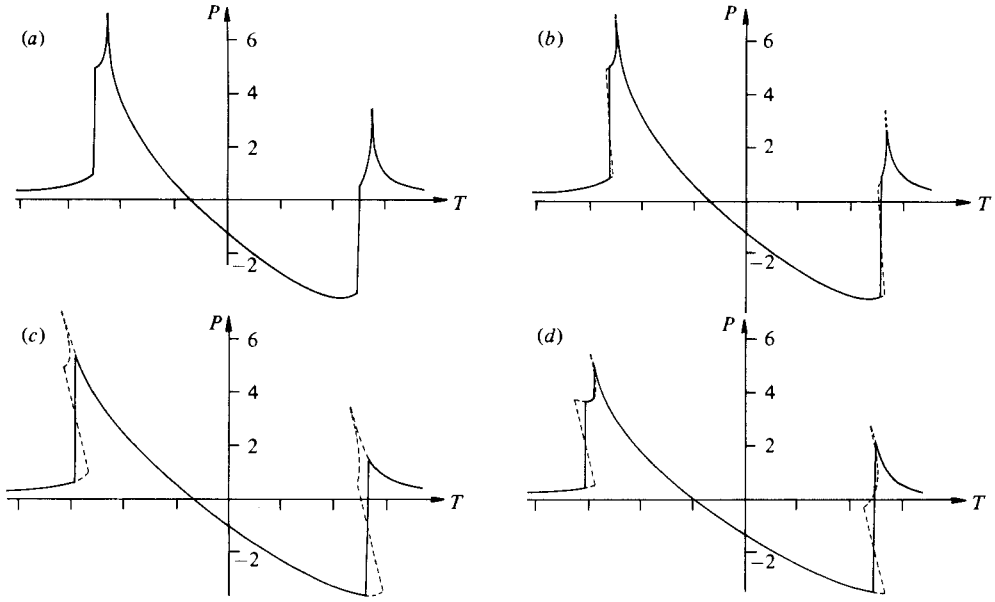

FIGURE 6. Pressure distributions in terms of physical coordinates: (*a*) $\epsilon = 0$, $X_1 = 0{\cdot}22$, $X_2 = 0$. $\beta = 0{\cdot}1$, $T_1/T_0 = 10^{-2}$; (*b*) 0·01, 0·22, 0, 0·1, 10^{-2}; (*c*) 0·02, 0·22, 0, 0·1, 10^{-2}; (*d*) 0·02, 0·3, 0, 0·1, 10^{-2}.

effects into approximately plane waves, a result which is very similar to one obtained already by Debye (1909) for converging waves of light near focal points. This special behaviour of the solution near the caustic then implies that the pattern of the 'shock waves' is not represented by a curve with a cusp at the caustic, as is suggested by geometric wave theories (see figure 1*a*), but by curves which look more like a Y and have triple points inside the caustics. This outcome is in accordance with experimental data published by Sanai, Toong & Pierce (1976).

(v) Outgoing solutions decay exponentially outside the caustic. Furthermore, as the high-frequency components of the signal decay faster than the low-frequency components, the pressure signatures become 'rounded', again a result caused by refraction effects.

4.2. *Physical coordinates*

To evaluate the actual solution we still have to replace the strained coordinates by physical coordinates. For that purpose we consider the following: at any particular point $\mathbf{X}_0$, the solution in strained coordinates may be given by the expressions derived above. For very small ϵ it is now obvious that the solutions in strained and in physical coordinates are approximately identical (figure 6*a*). If we increase the pressure amplitude ϵ, the transformation between real and strained coordinates displays an increasing steepening of the pressure signature in terms of real coordinates (dashed line in figure 6*b*). This steepening leads to multivalued solutions, which, however, are physically unrealistic. Therefore it becomes necessary to introduce shock fronts by suitable shock-fitting techniques (solid line in figure 6*b*). For our purposes the equal-area rule turns out to be appropriate, and is consistent with simplifications and approximations which we have introduced into the equations before.

An even further increase of ϵ leads, finally, to a steepening of the waves large enough that the shock fronts merge into a single shock wave (figure 6*c*). If we now keep ϵ

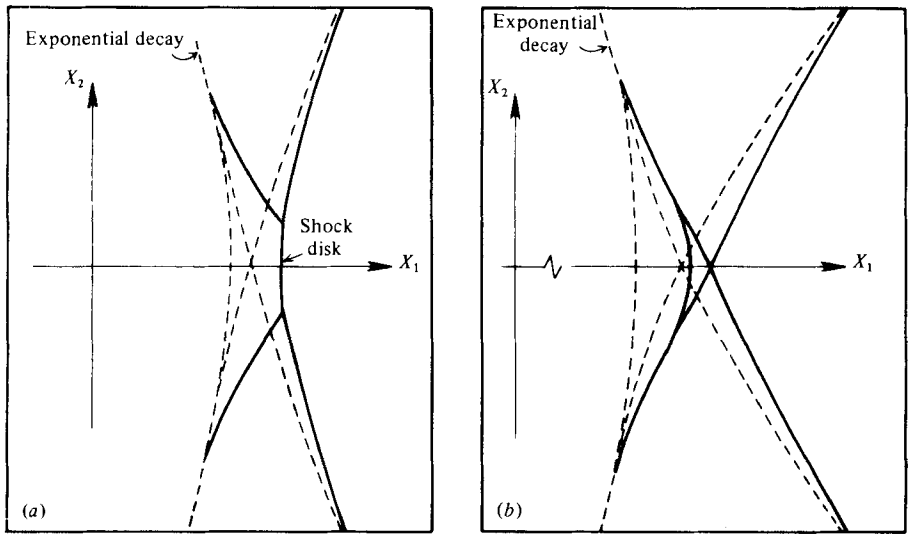

FIGURE 7. Shock pattern of the front wave according to strained coordinates (---) and to physical coordinates (——). (*a*) Mach shock or shock disk, (*b*) crossed shock waves.

constant, but move along the X_1 axis to higher values, the amplitude of the outgoing focused wave decreases and the distance between the waves increases. Then, even though the steepening also increases with growing travel distance, we finally reach a point on the X_1 axis where the shock-fitting technique in terms of physical coordinates no longer yields a single shock, but separated ones again (figure 6*d*).

Corresponding calculations are possible for other **X**-coordinates and varying ϵ-values. Based on these calculations, we may transform the time histories of the pressure field back into the **X**-plane. The resulting shock pattern of the leading wave system is shown qualitatively in figure 7.

In figure 7 (*a*), which corresponds to the pressure–time history shown in figure 6 (*c*), we realize that the solution yields a shock disk – also called a Mach shock – instead of three single shocks predicted by linear wave acoustics (equivalent to the solution in strained coordinates). However, if we move sufficiently far downstream (figure 7*b*), the shock-fitting technique no longer produces shock disks, but again crossover of shocks, i.e. folding of shocks reappears with a loop between the shocks. Nonetheless, the shock pattern itself still differs from the one obtained by the linear wave theory.

Finally, if we vary β but keep ϵ constant, we find that the point where the shock disks disappear moves upstream with increasing β (i.e. increasing curvature of S) and downstream with decreasing β (i.e. decreasing curvature of S).

These results agree very favourably with the experimental data obtained by Sturtevant & Kulkarny (1976) (see for instance their figure 7 and 18). The main quantitative differences between the experimental data and our theoretical method are based on the fact that the latter is restricted to only slightly curved incoming shock waves. In addition, our method is based on the assumption that the shock strength ϵ is at least smaller than 1, otherwise entropy effects become important, which we have neglected.

Until now, we confined the discussion to incident shock waves with very small but non-zero shock-rise times. In the following, those results are supplemented by the main results obtained for zero shock-rise time.

As we have mentioned before, the boundary conditions $T_1' > 0$ and $T_1' = 0$ at S are

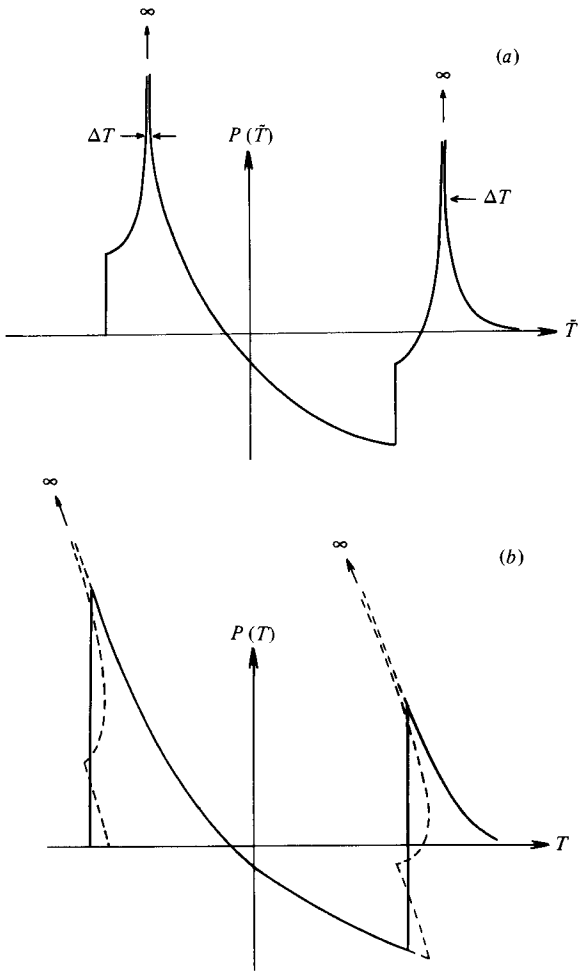

FIGURE 8. Qualitative sketch of shock fitting into pressure–time histories with singular peak amplitudes. (*a*) Solution according to strained coordinates, (*b*) solution according to physical coordinates.

equivalent from the physical point of view, while the first condition is preferable only because of its simpler algebra. Turning to the case $T_1' = 0$, one knows that the solution of a linear wave equation reveals singular behaviour for a focused pressure signal, i.e. the focused peaks of the signal behave either like $P \sim \ln(\Delta T)$ or $P \sim (\Delta T)^{-\alpha}$ with $0 < \alpha < 1$ depending upon the observation point. Furthermore, as we have elaborated before, the transformation (7) introducing the strained coordinates is determined in such a way that the nonlinear wave equation (6) in terms of real coordinates reduces to a formally linear wave equation (8) in terms of strained coordinates. Therefore that part of the solution which describes the focused wave shows singular behaviour for $T_1' = 0$ as well, which then leads to the question as to whether or not these singularities affect the solution in real coordinates as well.

The transformation (8*a*) from strained coordinates to real ones yields, for any particular shock strength $\epsilon > 0$, a multivalued solution like the one in figure 8(*b*), where the peak value and, consequently, the corresponding stretching of the coordinate, are infinitely large, but where the areas within the singular peaks remain

always finite. Therefore, the multivaluedness of the pressure signature can again be avoided by shock fronts fitted in according to the equal-area rule. The finiteness of the areas within the singular peaks now ensures that the location of the shock fronts (solid lines in figure 8*b*) and the maximum pressure amplitudes are very much the same whether one starts the calculation with the condition $T_1 > 0$ or $T_1 = 0$ at the surface S.

5. Conclusion

We have presented a mathematical approach which allows for the solution of a nonlinear wave equation for the pressure distribution in a flow field of weakly curved, converging shock waves, where the shock strength varies from weak to moderately strong. The method used describes sufficiently accurately the geometry of the shock pattern as a function of the shock strength, and it also describes correctly the nonlinear steepening effects of the flow behind the shocks. A still-open question is: How can one generalize the theory in a feasible way, or how can one develop an alternative approach to include non-planar, converging waves, which are no longer only weakly curved, but arbitrarily curved?

REFERENCES

Abramowitz, M. & Stegun, I. A. 1965 *Handbook of Mathematical Functions*. Dover.

Buchal, R. N. & Keller, J. B. 1960 *Communs Pure Appl. Math.* **13**, 85.

Cramer, M. S. & Seebass, A. R. 1978 *J. Fluid Mech.* **88**, 209.

Debye, P. 1909 *Ann. Physik* **30**, 755.

Fung, K.-Y. 1980 *SIAM J. Appl. Math.* **39**, 355.

Guiraud, J. P. 1965 *J. Méc.* **4**, 215.

Hayes, W. D. 1968 Similarity rules for nonlinear acoustic propagation through a caustic. In *Proc. 2nd Conf. on Sonic Boom Research. NASA* SP-180, p. 165.

Lighthill, M. J. 1950 *Q. J. Mech. Appl. Math.* **3**, 303.

Obermeier, F. 1976 Das Verhalten eines Überschallknalles in der Umgebung einer Kaustik. *Max-Planck-Inst. f. Strömungsforschung, Bericht* 28/1976.

Rott, N. 1980 *Z. Flugwiss.* **4**, 185.

Sanai, M., Toong, T.-Y. & Pierce, A. D. 1976 *J. Acoust. Soc. Am.* **59**, 513.

Seebass, A. R. 1971 Nonlinear acoustic behaviour at a caustic. In *Proc. 3rd Conf. on Sonic Boom Research. NASA* SP-255, p. 87.

Sturtevant, B. & Kulkarny, V. A. 1976 *J. Fluid Mech.* **73**, 651.

Vallee, J. 1969 Opération Jericho–Virage. *Rapport d'Etude* no. 277, *Centre d'Essais en Vol. Annexe d'Istres.*

Wanner, J. C. L., Vallee, J., Vivier, C. & Thery, C. 1972 *J. Acoust. Soc. Am.* **52**, 13.

Whitham, G. B. 1957 *J. Fluid Mech.* **2**, 145.

Whitham, G. B. 1959 *J. Fluid Mech.* **5**, 369.

Whitham, G. B. 1974 *Linear and Nonlinear Waves*. Wiley-Interscience.